Multispectral Image Dataset for Just Noticeable Difference Evaluation

Nenad Stojanović, Boban Bondžulić and Boban Pavlović

Military Academy, University of Defence in Belgrade,
Veljka Lukića Kurjaka 33, 11000 Belgrade, Serbia

e-mails: nenad.m.stojanovic@vs.rs, boban.bondzulic@va.mod.gov.rs, boban.pavlovic@va.mod.gov.rs

Abstract: This paper presents a new image dataset with the aim of expanding the possibilities to study the just noticeable differences in compressed images. To create the dataset, 35 images with three different visual appearances are used, two in the visible and one in the infrared part of the electromagnetic spectrum. The images in each domain show the same scene, and represent real outdoor environments. JPEG and BPG compression types are used. In total, the dataset includes 105 original images and 15960 compressed images. The dataset also contains data about subjectively determined boundaries of just noticeable differences in images. The procedure of collecting images and creating a complete dataset is described in the paper, along with the methodology used to conduct subjective tests. An analysis of the collected results was carried out. These data could be useful as training data for neural networks and deep learning model development, as well as for research on perceptually lossless compression. It is shown that BPG compression achieves, on average, a higher compression ratio than JPEG in all three considered cases. The highest compression degree is achieved with infrared images, which is shown through bit per pixel values. It has been shown that the compression ratio, efficiency of compression techniques, and objective image quality depend on the image content. The presented dataset is publicly available.

Keywords: just noticeable difference; multispectral images; visually lossless; JPEG; BPG

1 Introduction

Multimedia content is increasingly common in everyday life. Millions of images are posted daily on social networks and exchanged and shared through various transfer applications. Images in various formats and forms are widely used in medicine, space research, remote sensing, and other types of surveillance and monitoring. The information that can be gathered from just one image can be numerous. Additional information can be obtained through the processing of collected images. Thus, image processing has become increasingly present in

various applications. Real-time image processing algorithms, such as computer vision and various applications in artificial intelligence, have become extremely important.

One of the most common type of image processing is compression. Effective compression methods utilization becoming significantly important due to the increasing need to store a large number of visual contents. Also, there is a significant need to reduce the use of telecommunications resources or, in the case of communication channels, to release them quickly, as well as reduction of radio emissions.

Compression can be categorized into two basic types, lossless and lossy [1]. Some authors also introduce a derived compression type when perceptual signals are considered, named visually lossless [2]. Visually lossless compression represents lossy image compression without loss of visual quality. This sets a limit up to which the users cannot notice distortions caused by compression. This limit defines the term first Just Noticeable Difference (JND) point, which will be marked as JND#1. The JND#1 can be considered through different parameters that control the compression, number of bits per pixel (bpp), compression level, or various objective image quality assessment measures [3]. Determination of the first JND point can be divided into pixel-wise, patch-wise, and picture-wise. Compared to lossless compression techniques, an additional degree of compression of approximately eight times is achieved using a visually lossless approach [4].

Although the JPEG compression technique developed by the Joint Photographic Experts Group was created more than thirty years ago, it remains widely used today [5]. In addition to JPEG, a compression type that has the potential to push JPEG out of mainstream use is Better Portable Graphics (BPG) [6]. BPG originates from the H.265 video codec [7] as one of the modifications. This coder's advantage is its compression efficiency, which achieves high quality with minimal memory usage. BPG supports many different formats and color spaces and both lossless and lossy compression. Therefore, it is one of the highly promising compression coder [8].

Although more information can often be collected from an image rather from data collected from other types of sensors, observing a scene in only one spectral domain is sometimes insufficient. Major image sensors operate within visible part of the electromagnetic spectrum which includes wavelengths from 380 nm to 750 nm. However, this range may not always provide the necessary details. Wavelengths above 750 nm belong to the infrared (IR) part of the electromagnetic spectrum. The most frequently used part of the IR spectrum includes wavelengths of 0.75-14 μm. This part of the spectrum can be further divided into several sub-bands, but the 7.5-14 μm range is the most used in practice. This part of the IR spectrum is called long-wavelength infrared (LWIR) [9]. The image created in the LWIR part of the electromagnetic spectrum is a true thermal image. Thermal imaging can be defined as the receiving of IR radiation energy of the objects and background and the conversion of that radiation into an image [10].

This research was motivated by the need for high-quality image transmission using telecommunication channels with limited bandwidth. Determining JND#1 is highly significant in saving its resources. It enables the use of optimal memory capacity, optimal telecommunication channel capacity, or reduced transmission time in wireless communication systems.

The main contributions of this paper are:

- presentation of the first publicly available multispectral JND image dataset;
- expansion of the research field of determining the first JND point in images with compression into the multispectral domain, with specific application of IR images;
- comparative analysis of two widely used compression techniques in multispectral domain;
- availability of input data required for training of neural networks and development of deep learning and machine learning schemes for perceptually lossless image compression;
- development of object detection algorithms in multispectral domain.

An overview of the publicly available JND image datasets is presented in the second part of the paper. Subjective evaluation methods for the first JND point determination are also mentioned. In the third part, a new multispectral image dataset is presented. The fourth part of the paper describes the conducted subjective tests during the dataset creation. In the fifth part, the obtained results are analyzed. Finally, the concluding section summarizes the key findings.

2 Related Work

Research on detecting just noticeable differences in images with compression is a current research problem. The existence of image datasets with reference JND values is important for further research. Therefore, image datasets with the results of subjective evaluations are of great importance. Such datasets enable the development of objective algorithms for the fast, efficient, and automated prediction of the first JND point.

Now, there are already numerous datasets intended for researching JND for images with compression.

The Media Communications Lab – JND-based Coded Images (MCL-JCI) is the first dataset created for more detailed research of JPEG compression and the first JND point detection [11]. The dataset contains 50 original color images with High-Definition (HD) resolution. During testing, original and compressed images were

shown parallel. In addition to the first JND point, the determination of other JND points was carried out in this research. In [12], a dataset created of 202 original images in color and with HD resolution is presented. The type of compression of interest in this research is the video codec, known as Versatile Video Coding (H.266/VVC) [13], which was applied to still images.

The JPEG compression and first JND point on panoramic images are discussed in [14]. This dataset, named JND-Pano consists of 40 original color images. The images were shown parallel on a Head-Mounted Display (HMD) device. The detection of the first JND point in JPEG and WebP [15] compression types was analyzed in [16]. In addition to the above, the impact of viewing distance and illumination during display was also examined. Twenty HD color images were used to create this dataset. One-half of the images were compressed with WebP and the other half with the JPEG compression.

One small image dataset was presented to study JPEG compression and detection of the JND#1 in [17]. The dataset consists of 10 original color images with HD resolution. The Meikoudai Image Distortion Dataset (MIDD) image dataset, which is presented in [18], contains 10 original grayscale images. The JPEG, WebP, and High Efficiency Image Format (HEIF) [19] coders were used to create the complete dataset. The impact of the image resolution on the subjective detection of JND#1 was considered.

In contrast to, the previously mentioned datasets, where research was carried out in a laboratory, under strictly controlled conditions, the image datasets Konstanz Just Noticeable Difference 1k (KonJND-1k) [20], KonJND++ [21] and dataset described in [22] used crowdsourcing testing via the Internet. Also, another common feature of these datasets is that they contain a large number of original images. In the KonJND-1k, the impact of JPEG and BPG image compression on the determination of JND#1 was analyzed. The "flicker" method was used for subjective evaluation. In this method, the original and the compressed images appear alternately within the same window, and the subject notices the difference in quality by seeing the image change as a blink. The dataset KonJND++ deals with determining the regions where JND was observed, while the dataset from [22] considers many different types of degradations, among others JPEG and JPEG2000 codecs.

As seen from the previous, the two subjective methods for determining the first JND point are distinguished. Those two methods are "flicker" and side-by-side (parallel) display. Both methods can be subsumed under the double stimulus method. While there are no clearly defined standards for conducting such tests, it is essential to follow the guidelines established by the International Telecommunication Union (ITU) [23] regarding image selection, observation conditions, number of observers, and result analysis.

Two methods were selected for data collection. The first method is to collect opinions in a laboratory, under strictly controlled conditions, though this approach

is time-consuming. Another way of testing that has stood out and is becoming more and more attractive is crowdsourcing. Here, a large amount of data can be collected online in a much shorter time than in the laboratory, although the reliability of the results is lower. A detailed comparison of the advantages and disadvantages of these two testing environments can be found in [24].

To the best of our knowledge, the detection of the first JND point in compressed images within the same scene from multispectral domains has not been researched so far. The following chapters will present the results obtained after the realization of subjective tests on images with compression in both the visible and infrared spectral domains.

3 Image Dataset

The multispectral image dataset is created for the picture-wise first JND point detection and image compression research study. The dataset is created based on 105 (3×35) original images. It includes 35 color (CL), 35 grayscale (GR), and 35 infrared (IR) images. To create an image dataset, datasets that contain images of the same scene in the visible and LWIR range are considered.

Six images are selected from the eXtended Multispectral Dataset for Camouflage Detection (MUDCAD-X) dataset [25], consisting of three color images and three images from the LWIR part of the spectrum. The selected images correspond to the same scene with the resolution of 512×512 pixels. These images are captured using Unmanned Aerial Vehicle (UAV). Each image contains at least one object, often camouflaged.

Next 50 images (25 from visible and 25 from the LWIR part of the spectrum, all depicting the same scene) are selected from the Multi-scenario Multi-Modality (M^3FD) image dataset [26]. Resolutions of the images in this dataset vary, reaching up to 1024×768 pixels. Similar to the MUDCAD-X dataset, M^3FD also aims to study multispectral object detection and image fusion.

In the same manner, the authors captured images using the PTZ Dual-sensor Thermal Imaging Camera, model SHR-HVLV1000TIR104R. The acquisition was performed using the software package MATLAB and the images are stored in HD resolution. A total of seven color images and seven LWIR images are selected and added to the dataset.

Further, adequate adjustments were made. Image registration from different parts of the electromagnetic spectrum was performed. The images taken from the MUDCAD-X and M^3FD datasets have already been registered, and therefore only the images captured by the authors are registered through the manual selection of characteristic points.

Before applying grayscale compression, color images are converted into grayscale according to the expression [27]:

$$f(n,m) = 0.299R(n,m) + 0.587G(n,m) + 0.114B(n,m), \quad (1)$$

where R, G, and B are the red, green, and blue color components, respectively.

The JPEG and BPG compression types are used to complete the dataset creation. After registration, all images are cropped to dimensions that are a multiple of 32 pixels. The reason for this choice of image dimensions is the use of non-overlapping blocks for calculating the discrete cosine transform (DCT) and discrete sine transform (DST) in the BPG coder ensuring that edge effects due to incomplete blocks do not occur. The JPEG coder also meets this requirement due to 8×8 non-overlapping blocks for DCT calculation. The image resolutions in created dataset vary, ranging from 512×512 to 1920×1056 pixels. Different sensors for acquisition and different image resolutions make this dataset particularly challenging.

Furthermore, compression coders were applied to each original image in all three groups (color, grayscale, IR). For the JPEG compressed images subset, 100 additional images were created for each original image with different compression levels, for Quality Factor (QF) from 1 (high compression level) to 100 (low compression level). These images are generated using the MATLAB software package and the built-in *imwrite* function. A total of 10500 compressed images are created, 3500 for each group.

Unlike JPEG, BPG compression offers 52 compression levels, designated by a Quantization Parameter (QP) from 0 (low compression level) to 51 (high compression level) [20]. The images were created using the free BPGconv application, which can be downloaded from [28]. Compression was performed by selecting the following parameters within the application: compression level 9 (slow), chroma format 4:2:2, color space YCbCr, 8 bits depth and Joint Collaborative Team on Video Coding (JCTVC) HEVC encoder. A total of 5460 BPG compressed images are created.

The described dataset is named Just Noticeable Difference – Multispectral Image Dataset – Military Academy (JND-MID-MA) as a part of the research subject, images containing, and institution name of its creators. All images in the JND-MID-MA dataset are of outdoor type, with urban (23 images) and rural (12 images) environment. It opens possibilities for further research of object detection, surveillance, monitoring, and image fusion in real outdoor and multispectral environments with compressed images. Images from the MUDCAD-X dataset are marked with serial numbers 1 to 3, images from the M^3FD dataset have serial numbers 4 to 28, and images with serial numbers 29 to 35 are from authors archive. Several examples of same original images from presented JND-MID-MA image dataset in three domains are shown in Fig. 1. The JND-MID-MA image dataset is publicly available at the Mendeley Data repository [29] [30] [31].

img. no. 1 img. no. 8 img. no. 27 img. no. 30 img. no 34

Figure 1
Examples of original images from the created JND-MID-MA dataset

To show the variety of content and complexity of images from the dataset, the mean value of Spatial Information (SI_{mean}) [32] and the mean value of Spatial Frequency (SF_{mean}) [33] are calculated as numerical indicators. Additionally, Colorfulness (CF) [34] is considered for color images, while brightness is used for grayscale and IR images as numerical indicators of diversity.

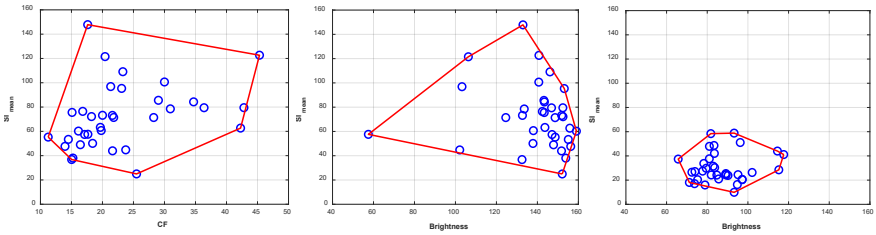

(a) (b) (c)

Figure 2
Distribution of SI_{mean} in relation to: (a) colorfulness for color original images; and brightness for (b) grayscale original images and (c) infrared original images

Fig. 2 shows scatter plots of the SI_{mean} in relation to colorfulness and brightness within convex hulls. For color images (Fig. 2(a)) and IR images (Fig. 2(c)) the distribution of values is quite uniform, with a slightly smaller number of images with higher CF and brightness values, respectively. For grayscale images (Fig. 2(b)), there is a significantly higher number of images with higher than lower brightness values. The SI_{mean} distribution is uniform across all three cases. It can be also observed that for IR images, SI_{mean} and brightness values have significantly lower dynamic ranges, compared to color and grayscale images. When SF_{mean} is observed in relation to CF and brightness, Fig. 3, a similar observation is achieved.

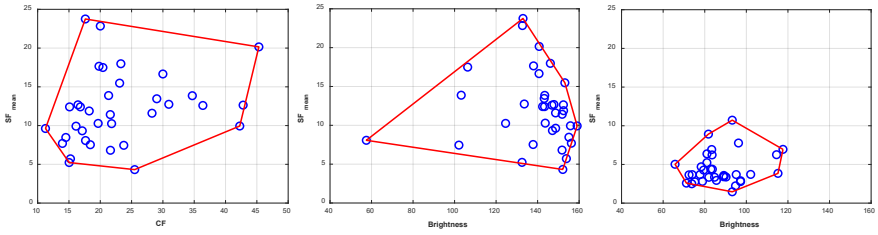

(a) (b) (c)

Figure 3

Distribution of SF_{mean} in relation to: (a) colorfulness for color original images; and brightness for (b) grayscale original images and (c) infrared original images

The image dataset was created in order to research the detection of the first JND point in images with different types of compression in the multispectral domain. The comprehensiveness of the presented dataset will support research into image processing in various areas, and one of the advantages of the dataset is that images of the same scene are registered. The subset of images in the infrared domain is particularly valuable, as it will significantly enhance research into the impact of standard compression coders on image quality in this part of the electromagnetic spectrum. It is also possible to expand the research into the effect of compression when applying image processing to other research areas, such as image fusion [35] and object detection [36].

4 Subjective Testing

Opinions about the first JND points in the JND-MID-MA image dataset are collected using specially developed software in MATLAB graphical user interface (GUI) environment. Subjective assessments were conducted in the laboratory under controlled conditions. One of the computer laboratories at the Military Academy was used as the testing facility. The laboratory was equipped with computers featuring 24-inch monitors, all set to HD resolution. During testing, participants assumed their usual computer workstation posture. This setup was chosen to gain insight into their visual experience within a relaxed, familiar environment. The tests were conducted under standard indoor lighting. Image presentation order during the test was randomized for each participant, which helped avoid fatigue effects. Each participant went through four parts of the test.

In the first part of the test, subjects are asked to answer several basic questions, such as first and last name, age, whether they wear eye corrections (glasses/lenses), and their level of knowledge regarding image processing and image compression principles.

Short instructions for the testing are given in the second part of the test. A few things are highlighted: there are no correct or incorrect answers, there is no time limit for responses and which degradation will deliver the used compression type. At the end of the instructional part, the subjects were trained in determining the first JND point using three test images.

The third part of the testing is the main part during which the first JND points are determined. Fig. 4 shows the window layout of the first JND point determination. The original and the compressed image are parallelly shown to the subjects. Using the binary search algorithm [11], the first JND points are determined. Subjects had to answer YES or NO to the question of whether they could notice the differences between the two displayed images. After the response, the image on the right side would change, with different compression levels, depending on the response. The first displayed compressed image is with half of the total value of the QF/QP (for JPEG QF=50, and BPG QP=26). Regardless of the test images' resolution, all images were displayed within the same window area. This setup allows for an additional analysis of the impact of image resolution when displayed on screens of limited size, such as smartphones or tablets.

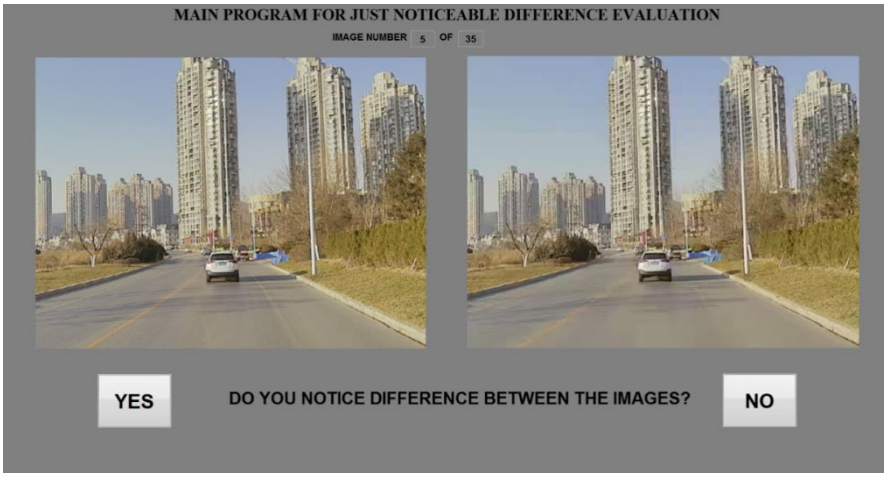

Figure 4
Window layout for the determination of the first JND point

In the fourth and last part, all participants are thanked for their participation after which the appropriate refreshments are provided.

5 Results and Discussion

Based on all of the above, the dataset can be divided according to compression type into JPEG and BPG and according to spectral bandwidths into visible and infrared, where color and grayscale images are considered for visible bandwidth. This classification results in six image subsets: JPEG-CL, JPEG-GR, JPEG-IR, BPG-CL, BPG-GR, and BPG-IR. A different number of observers participated in each subset of images. All observers were students (bachelor and doctoral students, and also course students from various units and institutions) and staff from the Military Academy, University of Defence in Belgrade, Republic of Serbia.

Subjects whose results differed significantly are removed as unreliable. Removal is done in four steps. In the first step, the mean value (μ) of the quality parameter (QF/QP) of JND#1 is calculated for each of the 35 images within each subset. In the second step, the standard deviation (σ) is determined. A dynamic range defined as [μ-σ, μ+σ] is designated. In the last step, all subjects who had more than 50% (for more than 18 images) JND#1 out of the designated range are rejected as unreliable. Tab. 1 provides an overview of the subjects who participated in testing across the image subsets. All subjects passed the Ishihara color blindness test. The data on age range, number of experts, and number of subjects with vision correction are derived from the pool of reliable participants. The experts included professors and doctoral students specializing in digital image processing, all familiar with infrared images. The final results of all JND#1 and standard deviations for all images by subsets can be found in [29] [30] [31].

Table 1
Data on subjects who participated in testing by subsets

Subset	JPEG					BPG				
	Participated (Male+Female)	Reliable (Male+Female)	Age range (Mean age)	Experts	Subjects with glasses/lenses	Participated (Male+Female)	Reliable (Male+Female)	Age range (Mean age)	Experts	Subjects with glasses/lenses
CL	33 (23+10)	26 (19+7)	21-45 (23.8)	5	6	31 (21+10)	29 (19+10)	21-36 (24.9)	4	7
GR	24 (17+7)	19 (14+5)	21-45 (24.7)	5	4	31 (21+10)	27 (19+8)	21-37 (24.8)	4	5
IR	29 (22+7)	22 (18+4)	21-45 (24.3)	5	4	31 (21+10)	27 (18+9)	21-37 (25.2)	4	6

Fig. 5 shows an example from the presented dataset. The left column shows the original images for all three cases. The middle column shows the images compressed with JPEG compression and subjectively determined as first JND points, with the given values of QF and the Peak Signal-to-Noise Ratio (PSNR) [37]. In the right column, there are BPG compressed JND#1 images. No obvious

visual differences are noticeable between the original and JND#1 images for either coder. PSNR values show that the images compressed using BPG coder exhibit slightly better (objective) quality of approximately 3 dB in all three cases.

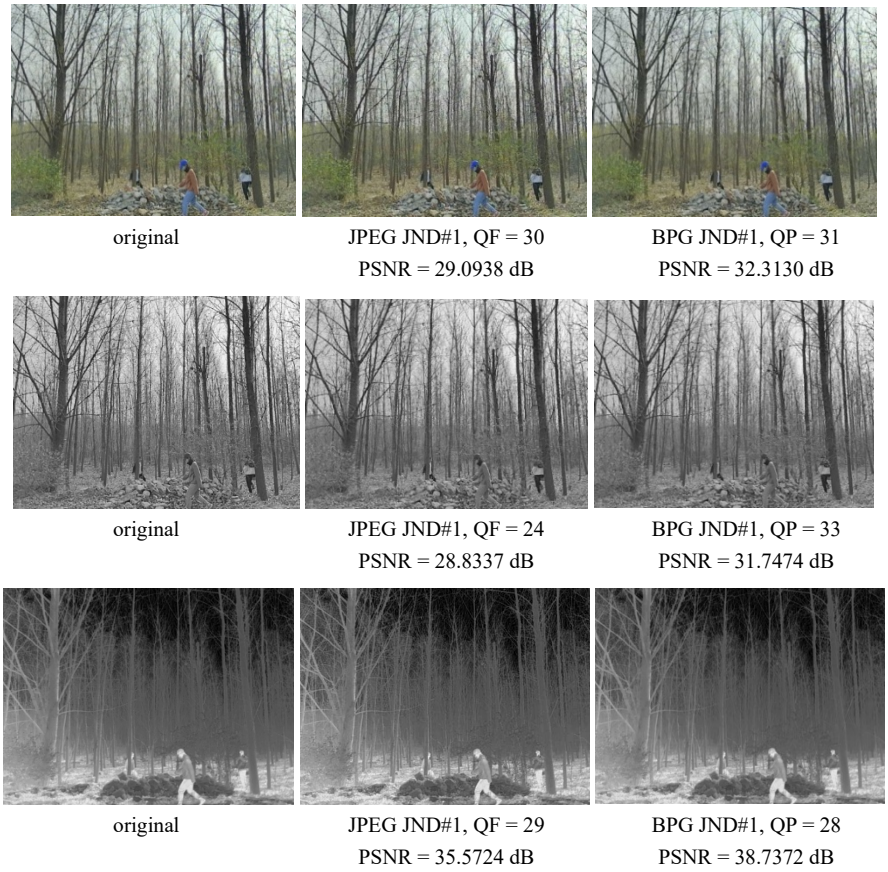

original	JPEG JND#1, QF = 30 PSNR = 29.0938 dB	BPG JND#1, QP = 31 PSNR = 32.3130 dB
original	JPEG JND#1, QF = 24 PSNR = 28.8337 dB	BPG JND#1, QP = 33 PSNR = 31.7474 dB
original	JPEG JND#1, QF = 29 PSNR = 35.5724 dB	BPG JND#1, QP = 28 PSNR = 38.7372 dB

Figure 5
Original and JND#1 compressed images from the JND-MID-MA dataset

The graphical representation of subjectively determined JND#1 points (QF/QP) is shown in Fig. 6. Fig. 6(a) presents the values obtained by applying JPEG compression, and Fig. 6(b) illustrates the results for BPG compression across all three considered cases. With JPEG JND#1 determined points, it can be observed that the values of color and grayscale images are quite similar, while the values of IR images differ slightly. In the case of BPG compression, images designated as JND#1 from the IR domain generally have lower QP values (lower degree of compression) compared to color and grayscale images.

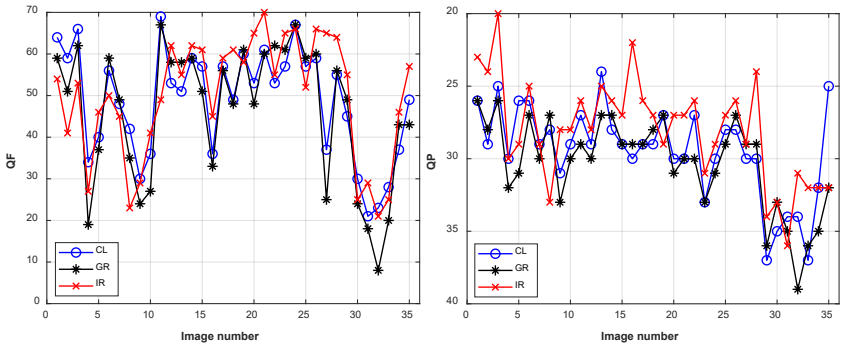

(a) (b)

Figure 6
JND#1 QF/QP values for (a) JPEG compression and (b) BPG compression

In order to better observe the relationship between the subjectively determined first JND points across the three considered cases, the Pearson linear correlation coefficient (PLCC) is calculated between them. The obtained PLCC scores are shown in Tab. 2. From the obtained results, it can be seen that for both compression methods, there is a stronger correlation between color and grayscale than in the other two cases. The QF/QP JND#1 values from the IR domain have a higher degree of agreement with grayscale images compared to color images. Furthermore, a greater degree of agreement between the first JND points can be observed with JPEG than with BPG compression.

Fig. 7 shows the PSNR values for the first JND images determined during the subjective tests. Three key observations are noticeable with both considered coders. First, color and grayscale images exhibit approximately similar objective quality. Second, IR images have better objective quality than color and grayscale images with a difference of 5-10 dB in most cases. The reason for this discrepancy may be the higher degree of homogeneity inherent to IR images compared to those from the visible spectrum, as well as the inherent blurriness of thermal images [38]. Third, and last, for image number eight there is a deviation, i.e. the objective quality of the IR image is lower compared to the other two cases for both coders. Examining the content of the eighth image in the dataset (Fig. 1), it can be seen that the visible part of the spectrum is obscured by smoke, masking details expressed in the IR image, therefore, this result could be expected.

Table 2
PLCC scores between QF/QP JND#1 values from the three considered cases

PLCC	JPEG	BPG
CL-GR	0.9494	0.7991
CL-IR	0.7418	0.6251
GR-IR	0.7701	0.7184

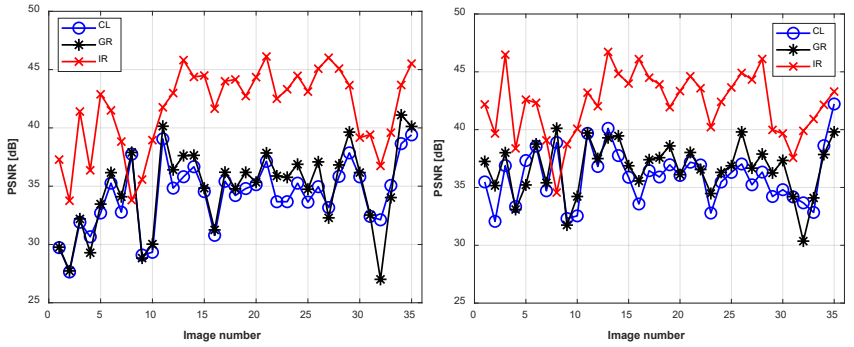

(a) (b)

Figure 7
PSNR JND#1 values for (a) JPEG compression and (b) BPG compression

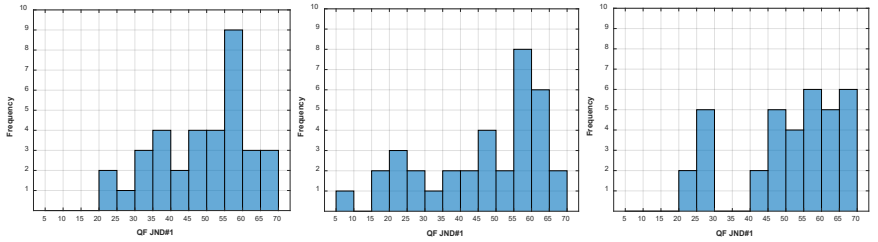

(a) (b) (c)

Figure 8
Histograms of QF JND#1 values for JPEG compression of (a) color, (b) grayscale and (c) infrared images

Fig. 8 shows the distribution of the first JND points for JPEG image subsets presented using histograms. The distribution of JND#1 for IR images, shows a greater concentration for higher QF values, with a gap between 30 and 40. For grayscale images, the first JND points are more concentrated within the QF range of 55 to 65. The distribution of JND#1 points for color images peaks in the range of 55 to 60, similar to grayscale images. Overall, the specified range that dominates represents images with a slightly lower degree of compression relative to the half-scale value (QF = 50).

Fig. 9 shows histograms of QP values for BPG image subsets. In all three cases, the distribution tends to follow a Gaussian, and a slightly higher number of JND#1 points are concentrated in the interval of QP values from 26 to 32, which represents images with a higher degree of compression relative to the half-scale value (QP = 26). It is interesting that the BPG coder does not have a large number of JND#1 images with QP values below 26.

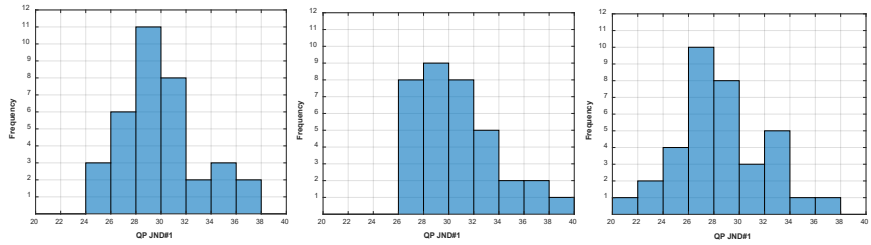

(a) (b) (c)

Figure 9
Histograms of QP JND#1 values for BPG compression of (a) color, (b) grayscale and (c) infrared images

Fig. 10 shows the bpp JND#1 values across all three image types and both coders. In general, it can be observed that BPG JND#1 compressed images have lower bpp values compared to those compressed using JPEG. This is not the case for images marked with numbers 1, 2, and 3, originating from the MUDCAD-X dataset. In addition to these three images, there are a few more exceptions in the color and grayscale subsets, but those differences in favor of JPEG are not pronounced. It can also be observed that the bpp values for IR images are lower than those for color and grayscale cases.

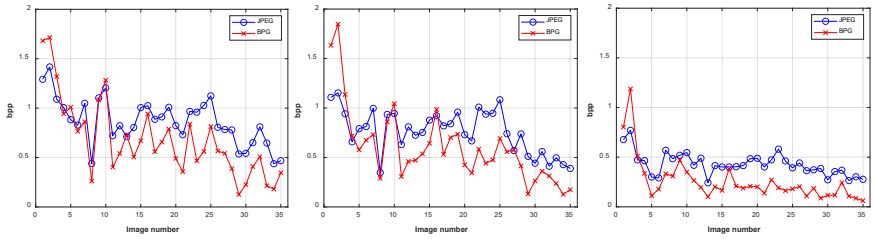

(a) (b) (c)

Figure 10
Values of bpp JND#1 images for (a) color, (b) grayscale and (c) IR image subsets

In accordance with what has been shown so far, Tab. 3 presents the minimum, maximum, and mean values for the quality parameter (QF/QP), PSNR, bpp and gain (G) for JND#1 images across all six image subsets. The numerical values confirm the previous observations. The mean values of QF/QP indicate that the compression level is slightly higher than half of the range. PSNR values indicate higher objective quality values for IR images. By observing bpp values, color and grayscale image subsets exhibit very similar bpp values with the BPG coder, unlike with the JPEG compression. In addition to the above, the gain was calculated as the ratio of the original image's file size to the JND#1 compressed image's file size. The highest gain is achieved with color image subsets. Compressed IR images yield higher gains

compared to grayscale images. Generally speaking, the statistical data shows that BPG compression achieves a larger gain compared to JPEG compression.

Table 3
Statistical values of quality parameters, PSNR and bpp for image subsets

Parameter		JPEG			BPG		
		CL	**GR**	**IR**	**CL**	**GR**	**IR**
QF/QP	Min	21	8	21	24	26	20
	Mean	48.514	46.171	49.914	29.457	30.286	28.029
	Max	69	67	70	37	39	36
PSNR [dB]	Min	27.640	27.007	33.751	32.070	30.362	34.563
	Mean	34.191	34.793	41.718	35.976	36.674	42.227
	Max	39.402	41.103	46.122	42.220	40.119	46.723
bpp	Min	0.437	0.347	0.242	0.126	0.128	0.062
	Mean	0.866	0.762	0.428	0.679	0.600	0.256
	Max	1.416	1.153	0.770	1.714	1.848	1.188
G	Min	16.943	6.939	10.391	13.998	4.330	6.736
	Mean	30.109	11.611	20.017	50.763	19.235	46.236
	Max	54.863	23.031	33.066	190.952	62.597	129.526

Further, the differences between two coders within the same domain can be analyzed by considering the mean bpp values. By observing color images, the BPG coder achieved a lower value of 0.187 bits per pixel compared to the JPEG coder. The BPG coder on this image subset achieves a mean compression ratio of 35.37 times, while JPEG reaches 27.73. Thus, the BPG coder achieves an average compression ratio 1.27 times higher than JPEG. BPG achieves an average compression ratio of 13.34 times, while for JPEG, this ratio is 10.49 for the grayscale image subset. This corresponds to an average compression ratio that is 1.27 times higher for BPG. Lastly, for the IR spectral band, the bpp difference is 0.17 in favor of BPG. Using JPEG, a compression ratio of 18.7 times is achieved. The BPG codec achieves a compression ratio of 31.24 times, which is 1.67 times higher than that of JPEG.

Quality analysis of JND#1 images is also performed using several full-reference objective image quality assessment measures. In addition to PSNR, Structural SIMilarity (SSIM) [39], PSNR-HVS-M [40], Haar wavelet-based perceptual similarity index (HaarPSI) [41], Deep Image Structure and Texture Similarity (DISTS) [42], and Local Standard Deviation-Based Image Quality (LSDBIQ) [43] are also employed. Fig. 11 shows the mean values of all JND#1 images by the subsets. PSNR, SSIM, and HaarPSI provide a significant advantage in objective quality to the BPG compression type (higher values are better). LSDBIQ also provides an advantage for images with BPG compression (lower values are better). Unlike these four objective measures, according to PSNR-HVS-M, the advantage in quality lies with JPEG compressed images. DISTS prefers BPG for color and

grayscale subsets, and JPEG is favored for the IR dataset. As JND#1 images correspond to the boundary between visually lossless and visually lossy compression, it can be concluded that the results of the LSDBIQ and DISTS objective measure best align with the results of subjective tests, since quality values with minimum differences are obtained for JPEG and BPG JND#1 compressed images in all three cases. Across all six tested image quality measures, the smallest difference occurs in the case of IR images.

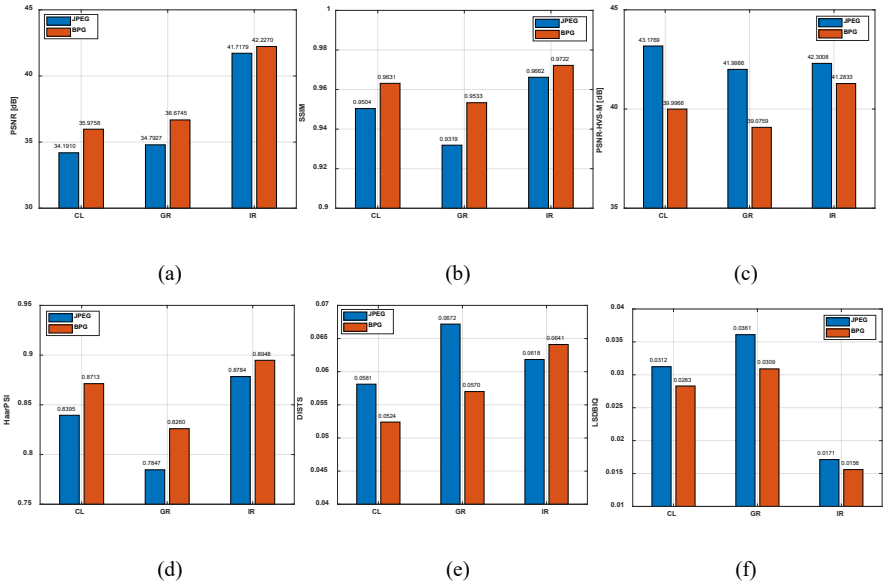

Figure 11

Mean values of objective image quality for JND#1 images obtained using (a) PSNR, (b) SSIM, (c) PSNR-HVS-M, (d) HaarPSI, (e) DISTS and (f) LSDBIQ

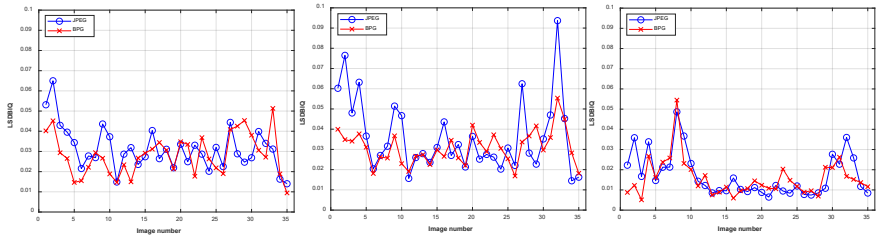

Figure 12

LSDBIQ values of JND#1 images for (a) color, (b) grayscale and (c) IR image subsets

LSDBIQ measure is developed for the quality evaluation of compressed images. Fig. 12 shows LSDBIQ values for the first JND images in the presented dataset. It

can be seen that the quality is very similar for IR images (Fig. 12(c)), with only a few instances where the objective quality leans toward the BPG coder. For shade, bigger difference in objective LSDBIQ quality for each image was obtained for color images (Fig. 12(a)), while the biggest difference was obtained for grayscale images (Fig. 12(b)). It is noticeable that in the case of a few images where a significant difference in LSDBIQ values is obtained, it is in most cases in favor of BPG. This ultimately results in an average quality value that favors BPG.

Conclusions

A novel image dataset, named JND-MID-MA, for just noticeable difference research, is presented in the paper. The dataset contains color, grayscale, and infrared original images of the same scene, which are additionally degraded with two compression types. The tests are conducted using the picture-wise double stimulus method. The dataset is very challenging for research as it contains images from three different datasets, from three domains, and images vary in resolution.

Comparing the two used compression techniques, it is shown that with BPG, on average, a 1.27 higher compression ratio was achieved for color and grayscale subsets, and 1.67 for infrared subset, compared to JPEG, based on mean bpp values. However, by observing each image individually, it can be concluded that the usage of the optimal compression coder depends on several factors, such as the content and complexity of the image or the sensor that collects the data.

The LSDBIQ and DISTS image quality assessment measures have the potential to be used as objective visibility metrics for visually lossless, both JPEG and BPG image compression.

In future work, development of an objective method for JND#1 detection is planned. JND#1 prediction will be based on simple image features. Feature importance analysis, using tools such as Random Forest, SHapley Additive exPlanations (SHAP) values, Particle Swarm Optimization (PSO), or similar, is also planned to improve single feature-based prediction. The prediction would be performed through various image quality assessment metrics. Ultimately, this process would provide a recommendation for the image features and image quality assessment metric to be used for prediction.

Also, in further research, it is planned to collect subjective opinions about the position of JND#1 by using crowdsourcing and comparing the collected results with the results presented in this work, with the appropriate adaptation of the existing software for working via the Web.

List of abbreviations and notations

BPG	*Better Portable Graphics*
BPG-CL	*Subset of Color BPG Compressed Images*
BPG-GR	*Subset of Grayscale BPG Compressed Images*
BPG-IR	*Subset of Infrared BPG Compressed Images*
bpp	*bits per pixel*
CF	*Colorfulness*

CL	*Color*
DCT	*Discrete Cosine Transform*
DISTS	*Deep Image Structure and Texture Similarity*
DST	*Discrete Sine Transform*
G	*Gain*
GR	*Grayscale*
GUI	*Graphical User Interface*
H.266/VVC	*Versatile Video Coding*
HaarPSI	*Haar wavelet-based Perceptual Similarity Index*
HD	*High-Definition*
HEIF	*High Efficiency Image Format*
HEVC	*High Efficiency Video Coding*
HMD	*Head-Mounted Display*
IR	*Infrared*
ITU	*International Telecommunication Union*
JCTVC	*Joint Collaborative Team on Video Coding*
JND	*Just Noticeable Difference*
JND#1	*First Just Noticeable Difference Point*
JND-MID-MA	*Just Noticeable Difference–Multispectral Image Dataset–Military Academy*
JND-Pano	*Panoramic Image Dataset*
JPEG	*Joint Photographic Experts Group*
JPEG-CL	*Subset of Color JPEG Compressed Images*
JPEG-GR	*Subset of Grayscale JPEG Compressed Images*
JPEG-IR	*Subset of Infrared JPEG Compressed Images*
LSDBIQ	*Local Standard Deviation-Based Image Quality*
LWIR	*Long-Wavelength Infrared*
KonJND-1k	*Konstanz Just Noticeable Difference 1k*
MCL-JCI	*Media Communications Lab – JND-based Coded Images*
MDID	*Meikoudai Image Distortion Dataset*
MUDCAD-X	*eXtended Multispectral Dataset for Camouflage Detection*
M^3FD	*Multi-scenario Multi-Modality*
QF	*Quality Factor*
QP	*Quantization Parameter*
PLCC	*Pearson Linear Correlation Coefficient*
PSNR	*Peak Signal-to-Noise Ratio*
PSNR-HVS-M	*Peak Signal-to-Noise Ratio – Human Visual System – Masking*
PSO	*Particle Swarm Optimization*
SF	*Spatial Frequency*
SHAP	*SHapley Additive exPlanations*
SI	*Spatial Information*
SSIM	*Structural Similarity Index*
UAV	*Unmanned Aerial Vehicle*
σ	*Standard Deviation*
μ	*Mean Value*

Acknowledgment

This research has been a part of the project No. VA-TT/1/25-27 supported by the Ministry of Defence, Republic of Serbia.

References

[1] Hussain, A. J., Al-Fayadh, A., Radi, N.: Image compression techniques: A survey in lossless and lossy algorithms, Neurocomputing 300, 2018, pp. 44-69, doi: 10.1016/j.neucom.2018.02.094

[2] Kryvenko, L., Krylova, O., Lukin, V., Kryvenko, S.: Intelligent visually lossless compression of dental images, Advanced Optical Technologies, 2024, Vol. 13, 1306142, doi: 10.3389/aot.2024.1306142

[3] Liu, H., Zhang, Y., Zhang, H., Fan, C., Kwong, S., Jay Kuo, C.-C., Fan, X.: Deep learning-based picture-wise just noticeable distortion prediction model for image compression, IEEE Transactions on Image Processing, 2020, Vol. 29, pp. 641-656, doi: 10.1109/TIP.2019.2933743

[4] Bondžulić, B., Lukin, V., Bujaković, D., Li, F., Kryvenko, S.: On visually lossless JPEG image compression, in IEEE Proceedings of the Zooming Innovation in Consumer Technologies Conference (ZINC), Novi Sad, Serbia, 2023, pp. 113-118, doi: 10.1109/ZINC58345.2023.10174090

[5] Hudson, G., Léger, A., Niss, B., Sebestyén, I., Vaaben, J.: JPEG-1 standard 25 years: past, present, and future reasons for a success, Journal of Electronic Imaging, 2018, Vol. 27, No. 4, pp. 040901-1-040901-19, doi: 10.1117/1.JEI.27.4.040901

[6] https://bellard.org/bpg/ (last accessed 05.12.2024)

[7] High Efficiency Video Coding, document ITU-T H.265/ISO/IEC 23008-2 HEVC, 2023, https://www.iso.org/standard/85457.html

[8] Wang, Y., Mukherjee, D.: The discrete cosine transform and its impact on visual compression: fifty years from its invention [perspectives], IEEE Signal Processing Magazine, 2023, Vol. 40, No. 6, pp. 14-17, doi: 10.1109/MSP.2023.3282775

[9] Perić, D., Livada, B., Perić, M., Vujić, S.: Thermal imager range: Predictions, expectations and reality, Sensors, 2019, Vol. 19, No. 15, p. 3313, doi: 10.3390/s19153313

[10] Hou, F., Zhang, Y., Zhou, Y., Zhang, M., Lv, B., Wu, J.: Review on infrared imaging technology, Sustainability, 2022, Vol. 14, No. 18, p. 11161, doi: 10.3390/su141811161

[11] Jin, L., Lin, J. Y., Hu, S., Wang, H., Wang, P., Katsavounidis, I., Aaron, A., Kuo, C.-C. J.: Statistical study on perceived JPEG image quality via MCL-JCI dataset construction and analysis, in Proceedings IS&T International Symposium on Electronic Imaging – Image Quality and System Performance XIII, San Francisco, CA, USA, 2016, Article no. IQSP-222, doi: 10.2352/ISSN.2470-1173.2016.13.IQSP-222

[12] Shen, X., Ni, Z., Yang, W., Zhang, X., Wang, S., Kwong, S.: A JND dataset based on VVC compressed images, in Proc. IEEE International Conference on Multimedia & Expo Workshop, London, United Kingdom, 2020, pp. 1-6, doi: 10.1109/ICMEW46912.2020.9105955

[13] ITU: Versatile video coding, Recommendation ITU-T H.266 (V3) (09/2023), International Telecommunication Union Geneva, Switzerland, 2023

[14] Liu, X., Chen, Z., Wang, X., Jiang, J., Kwong, S.: JND-Pano: database for just noticeable difference of JPEG compressed panoramic images, Lecture Notes in Computer Science, 2018, Vol. 11164, pp. 458-468, doi: 10.1007/978-3-030-00776-8_42

[15] https://developers.google.com/speed/webp/ (last accessed 05.12.2024)

[16] Mikhailiuk, A., Ye, N., Mantiuk, R. K.: The effect of display brightness and viewing distance: a dataset for visually lossless image compression, Electronic Imaging, 2021, Vol. 33, No. 11, pp. 152-1-152-8, doi: 10.2352/ISSN.2470-1173.2021.11.HVEI-152

[17] Afnan, U. F., Yaseen, L. J., Jamil, S., Kwon, O.: Subjective assessment of objective image metrics range guaranteeing visually lossless compression, 2023, Sensors, Vol. 23, No. 3, p. 1297, doi: 10.3390/s23031297

[18] Honda, S. Maeda, Y., Fukushima, N.: Dataset of subjective assessment for visually near-lossless image coding based on just noticeable difference, in Proceedings 15th International Conference on Quality of Multimedia Experience (QoMEX), Ghent, Belgium, 2023, pp. 236-239, doi: 10.1109/QoMEX58391.2023.10178524

[19] Lainema, J., Hannuksela, M. M., Vadakital, V. K. M., Aksu, E. B.: HEVC still image coding and high efficiency image file format, in Proceedings IEEE International Conference on Image Processing (ICIP), Phoenix, AZ, USA, 2016, pp. 71-75, doi: 10.1109/ICIP.2016.7532321

[20] Lin, H., Chen, G., Jenadeleh, M., Hosu, V., Reips, U. D., Hamzaoui, R., Saupe, D.: Large-scale crowdsourced subjective assessment of picturewise just noticeable difference, IEEE Transactions on Circuits and Systems for Video Technology, 2022, Vol. 32, No. 9, pp. 5859-5873, doi: 10.1109/TCSVT.2022.3163860

[21] Chen, G., Lin, H., Wiedemann, O. Saupe, D.: Localization of just noticeable difference for image compression, in Proceedings 15th International Conference on Quality of Multimedia Experience (QoMEX), Ghent, Belgium, 2023, pp. 61-66, doi: 10.1109/QoMEX58391.2023.10178653

[22] Liu, Y., Jin, J., Xue, Y., Lin, W.: The first comprehensive dataset with multiple distortion types for visual just-noticeable differences, in Proceedings International Conference on Image Processing (ICIP), Kuala Lumpur, Malaysia, 2023, pp. 2820-2824, doi: 10.1109/ICIP49359.2023.10221977

[23] ITU: Methodologies for the subjective assessment of the quality of television images, Recommendation ITU-R BT. 500-14 (10/2019), International Telecommunication Union Geneva, Switzerland, 2019

[24] Testolina, M., Ebrahimi, T.: Review of subjective quality assessment methodologies and standards for compressed images evaluation, in Proceedings Applications of Digital Image Processing XLIV, SPIE, 2021, Vol. 11842, pp. 302-315, doi: 10.1117/12.2597813

[25] Hupel, T., Stütz, P.: Measuring and predicting sensor performance for camouflage detection in multispectral imagery, Sensors, 2023, Vol. 23, No. 19, 8025, doi: 10.3390/s23198025

[26] Liu, J., Fan, X., Huang, Z., Wu, G., Liu, R., Zhong, W., Luo, Z.: Target-aware dual adversarial learning and a multi-scenario multi-modality benchmark to fuse infrared and visible for object detection, in Proceedings of the IEEE/CVF Conference on Computer Vision and Pattern Recognition, New Orleans, LA, USA, 2022, pp. 5802-5811, doi: 10.1109/CVPR52688.2022.00571

[27] Gonzalez, R. C., Woods, R. E.: Digital Image Processing, 4th ed., London: Pearson Education, 2018, ISBN 13: 978-1-292-22304-9

[28] https://bpgconv.software.informer.com/ (last accessed 05.12.2024.)

[29] Stojanović, N., Bondžulić, B.: JND-IR image dataset, Mendeley Data, V1, 2024, available at: https://data.mendeley.com/datasets/x79wx5fz6b/1

[30] Stojanović, N., Bondžulić, B.: JND-TV image dataset, Mendeley Data, V1, 2024, available at: https://data.mendeley.com/datasets/537w5jhb7s/1

[31] Stojanović, N., Bondžulić, B.: JND-GR image dataset, Mendeley Data, V1, 2024, available at: https://data.mendeley.com/datasets/vzzgr62brk/1

[32] Korhonen, J., Reiter, U., Ukhanova, A.: Frame rate versus spatial quality: Which video characteristics do matter?, in Proceedings of the IEEE Visual Communications and Image Processing (VCIP), Kuching, Malaysia, 2013, pp. 1-6, doi: 10.1109/VCIP.2013.6706381

[33] Tan, W., Zhou, H. X., Yu, Y., Du, J., Qin, H. Ma, Z., Zheng, R.: Multi-focus image fusion using spatial frequency and discrete wavelet transform, in Proceedings of Applied Optics and Photonics China 2017: Optical Sensing and Imaging Technology and Applications, SPIE, Vol. 10462, Beijing, China, 2017, pp. 1215-1225, doi: 10.1117/12.2285561

[34] Hasler, D., Suesstrunk, S. E.: Measuring colourfulness in natural images, in Proceedings of Human Vision and Electronic Imaging VIII, SPIE 5007, Santa Clara, CA, USA, 2003, pp. 87-95, doi: 10.1117/12.477378

[35] Xing, M., Liu, G., Tang, H., Qian, Y., Zhang, J.: CFNet: An infrared and visible image compression fusion network, Pattern Recognition, 2024, Vol. 156, 110774, doi: 10.1016/j.patcog.2024.110774

[36] Deguerre, B., Chatelain, C., Gasso, G.: Fast object detection in compressed JPEG images, in Proceedings of the IEEE Intelligent Transportation Systems

Conference (ITSC), Auckland, New Zealand, 2019, pp. 333-338, doi: 10.1109/ITSC.2019.8916937

[37] Wang, Z., Bovik, A. C.: Mean squared error: Love it or leave it? A new look at signal fidelity measures, IEEE Signal Processing Magazine, 2009, Vol. 26, No. 1, pp. 98-117, doi: 10.1109/MSP.2008.930649

[38] Bao, F., Jape, S., Schramka, A., Wang, J., McGraw, T. E., Jacob, Z.: Why thermal images are blurry, Optics Express, 2024, Vol. 32, No. 3, pp. 3852-3865, doi: 10.1364/OE.506634

[39] Wang, Z., Bovik, A. C., Sheikh, H. R., Simoncelli, E. P.: Image quality assessment: From error visibility to structural similarity, IEEE Transactions on Image Processing, 2004, Vol. 13, No. 4, pp. 600-612, doi: 10.1109/TIP.2003.819861

[40] Ponomarenko, N., Silvestri, F., Egiazarian, K., Carli, M., Astola, J., Lukin, V.: On between-coefficient contrast masking of DCT basis functions, in Proceedings of the Third International Workshop on Video Processing and Quality Metrics for Consumer Electronics VPQM-07, Scottsdale, Arizona, USA, 2007, available at: http://sp.cs.tut.fi/pubdl/Ponomarenko2007-On.pdf

[41] Reisenhofer, R., Bosse, S., Kutyniok, G., Wiegand, T.: A Haar wavelet-based perceptual similarity index for image quality assessment, Signal Processing: Image Communication, 2018, Vol. 61, pp. 33-43, doi: 10.1016/j.image.2017.11.001

[42] Ding, K., Ma, K., Wang, S., Simoncelli, E. P.: Image quality assessment: Unifying structure and texture similarity, IEEE Transactions on Pattern Analysis and Machine Intelligence, 2022, Vol. 44, No. 5, pp. 2567-2581, doi: 10.1109/TPAMI.2020.3045810

[43] Gore, A., Gupta, S.: Full reference image quality metrics for JPEG compressed images, AEU-International Journal of Electronics and Communications, 2015, Vol. 69, No. 2, pp. 604-608, doi: 10.1016/j.aeue.2014.09.002